Reservoir Geometry Determination and Volumetric Reserve Estimation of an Offshore, Niger Delta Basin Nigeria

ABSTRACT

Volumetric reserve estimation had been carried out as well as deducing the reservoir geometry of Idje field. Idje field is an 8.4 km^2 area between latitudes $4^o31'49"N$ and 4^o 33'23" N and longitudes $4^o34'43"E$ and $4^o36'17"E$ offshore Niger Delta in a water depth of approximately 1000m on the continental slope. Well, logs suites from ten wells comprising gamma-ray, resistivity, neutron and density were obtained and analyzed. From the result, it was observed that the reservoir was a sedimentary dome possibly resulting from an underlying shale diaper. The volumetric reserve estimate for the D-3 reservoir shows that it contains 15.8 million barrels of oil and 32 billion cubic feet of gas. If the field is produced at the rate of 10,000 barrels per day, it would yield production for approximately 4 years before subsequent secondary and tertiary recovery measures would be employed.

1. INTRODUCTION

Proper understanding of the underlying geology helps to accurately predict the hydrocarbon potentials and reserves estimation of a petroleum field. Information gathered from cores, seismic, well logs and biostratigraphic data help to resolve this underlying geology and thus aid in characterizing the hydrocarbon reservoir. Reservoir characterization, therefore, is the quantification, integration, reduction and analysis of geological, petrophysical, seismic and engineering data. Reservoirs in the Niger Delta exhibit a wide range of complexities in their sedimentological and petrophysical characteristics due to differences in hydrodynamic conditions prevalent in their depositional settings. Petrophysics, therefore, plays a fundamental role in the description, characterization and evaluation of reservoirs. It is always essential to integrate petrophysical data with geological and engineering data to accurately predict reservoir quality. Reserve estimation, therefore, is based on the field wide distribution of these reservoir properties. Due to the intense petroleum exploration and exploitation activities in the Niger Delta region during the last two decades, a vast amount of data have been accumulated from which it had been possible to establish the historical reconstruction and evolution of the Niger Delta basin (Short and Stauble, 1967; Avbovbo, 1978).

Ten wells were drilled in the Idje field to produce the D-3 reservoir; Idje 2, 3 and 10 penetrated the gas and oil zones; Idje 1 penetrated only the oil zone. Idje 4 and 6 penetrated the fringe of the reservoir while Idje 5, 7, 8 and 9 are dry wells which penetrated only the water zone. Well, logs were obtained and correlated across the D-3 reservoir. Also, the petrophysical characteristic of the D3 reservoir was determined. Increased confidence in the reservoir characterization and architecture is provided by the integration of a large number of data on well. The goal of this study is to provide a better understanding of the distribution pattern of the reservoir properties across the field.

1.1 Study Location

Idje is a fictitious field name given to an 8.4 km^2 area between latitudes $4^o31'49"N$ and 4^o 33'23" N and longitudes $4^o34'43"E$ and $4^o36'17"E$ offshore Niger Delta in a water depth of approximately 1000m on the continental slope and it lies at approximately 170km southwest of Warri as seen in Fig. 1. and Fig. 2 respectively.

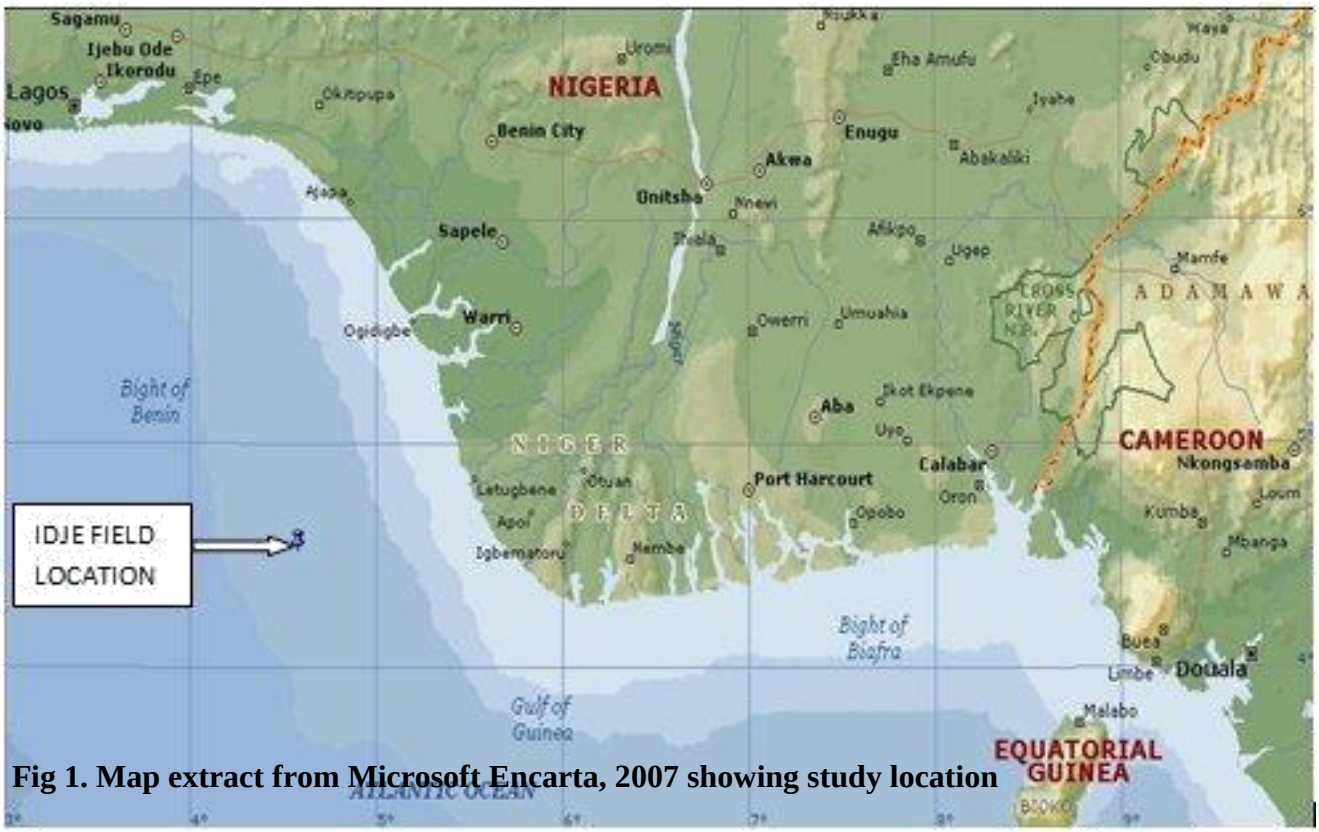

Fig 1. Map extract from Microsoft Encarta, 2007 showing study location

Fig. 2 Map extract from Google Earth showing project location on the continental slope.

1.2 The **Niger Delta Regional Setting**

The Niger Delta covers a 70,000 square kilometre area within the Gulf of Guinea, West Africa. Although the modern Niger Delta formed in the Early Tertiary, sediments began to accumulate in this region during the Mesozoic rifting associated with the separation of Africa and South American continents (Weber and Daukoru, 1975; Evamy *et al*, 1978; Doust and Omatsola, 1990). Synrift marine clastics and carbonates accumulated during a series of transgressive and regressive phases between the Cretaceous to Early Tertiary; the oldest dated sediments are Albian (Doust and Omatsola, 1990). These synrift phases ended with basin inversion in the Late Cretaceous (Santonian). Proto-Niger Delta regression continued as continental margin subsidence resumed at the end of the Cretaceous (Maastrichtian). Niger Delta progradation into the Gulf of Guinea accelerated from the Miocene onward in response to evolving drainages of the River Niger, River Benue and Cross River and continued continental margin subsidence. Tertiary Niger Delta deposits are characterized by a series of depobelts that strike northwest-southeast, subparallel to the present-day shoreline. Depobelts become successively younger basinward, ranging in age from Eocene in the north to Pliocene offshore of the present shoreline. Depobelts, tens of kilometres wide, is bounded by a growth fault to the north and a counter regional fault seaward. Each sub-basin contains a distinct shallowing upward depositional cycle with its tripartite assemblage of marine, paralic, and continental deposits. Depobelts define a series of punctuations in the progradation of this deltaic system. As deltaic

sediment loads increase, underlying delta front and pro-delta marine shale begin to move upward and basinward. Mobilization of basal shale caused structural collapse along normal faults and created accommodation for additional deltaic sediment accumulation. As shale withdrawal nears completion, subsidence slows dramatically, leaving little room for further sedimentation. As declining accommodation forces a basinward progradation of sediment, a new depocenter develops basinward. Most Niger Delta faulting is due to extensional deformation. The exception is in the distal section, where overthrust faults form in the toe of the proto-Niger delta. These extensional faults are normal and generally listric, comprising syndepositional growth faults and crustal tensional relief faults. These faults are synthetic or antithetic, running sub-parallel to the strike of the sub-basins. These synsedimentary faults exhibit growth strata above the downthrown block, as well as anticlinal (rollover) closures. Most hydrocarbon-bearing structures in Niger Delta deposits are close to these structure-building faults, in the complexly collapsed crest and faulted anticlinal structures. Growth faults and antithetic faults play an essential role in trap configuration. Growth fault exhibit significant throw (up to several hundred meters) are arcuate in plain view, concave basinward and maybe several tens of kilometres in length.

1.3 Formations And Depositional Environments

The morphology of the Niger Delta changed from an early stage, spanning the Paleocene to Early Eocene, to a later stage of delta development beginning in Miocene time. Early coastlines were concave to the sea and depositional patterns were strongly influenced by basement topography (Doust and Omatsola, 1990). Delta progradation occurred along two major axes. The first paralleled the Niger River, where sediment supply exceeds subsidence rate. The second, smaller than the first, became active basinward of the Cross River during the Eocene to Early Oligocene. Late stages of deposition began in the Early to Middle Miocene, as these separate eastern and western depocenters merged. In late Miocene, the delta prograded far enough that shorelines became broadly concave into the basin. Accelerated loading by this rapid delta progradation mobilized underlying unstable shales. These shales rose into diapiric walls, deforming overlying strata. The resulting complex deformation structures caused local uplift, which resulted in major erosion events into the leading progradational edge of the Niger Delta. Several deep canyons, now clay-filled, cut into the shelf are commonly interpreted to have formed during sea-level low stands. The best known are the Afam, Opuama, and Qua Iboe Canyon fills (Reijers *et al*, 1997 and Tuttle *et al*, 1999).

Short and Stauble (1967) defined formations within the Niger Delta clastic wedge based on sand/shale ratios estimated from subsurface well logs. The three major lithostratigraphic units defined in the subsurface of Niger Delta Akata, Agbada and Benin Formations reflect a gross upward-coarsening clastic wedge. These Formations were deposited in dominantly marine, deltaic and fluvial environments, respectively (Weber and Daukoru, 1975; Weber, 1987). Stratigraphically equivalent units to these three formations are exposed in southern Nigerian (Short and Stauble, 1967).

The Akata Formation occurs as pro-deltaic dark grey shales and silts with rare streaks of sand of probable turbidite flow origin, is estimated to be 6,400m thick in the central part of this clastic wedge (Short and Stauble, 1967); (Doust and Omatsola, 1990). Marine planktonic foraminifera suggests a shallow marine shelf depositional setting ranging from Paleocene to Recent in age (Doust and Omatsola, 1990; Whiteman, 1982). These shales are exposed onshore in the northeastern part of the delta, where they are referred to as the Imo shale. This formation also crops out offshore in diapers along the continental slopes, where deeply buried, Akata shales are typically overpressured. Akata shales have been interpreted to be pro-delta and deeper water deposits that shoal vertically into the Agbada Formation (Stacher, 1995; Doust and Omatsola, 1990). It is thought to be the source rock of the Niger delta complex.

The Agbada Formation occurs as a paralic sequence of shale and sand interbeds throughout the Niger Delta clastic wedge. It increases in shale thickness and decreases in sand thickness with depth. It has a maximum thickness of about 3,900m and ranges in age from Eocene to Pleistocene (Doust and Omatsola, 1990). It crops out in southern Nigeria, where it is called the Ogwashi-Asaba and Ameki Formations respectively. The lithologies consist largely of alternating sands, silts and shales with progressive upward changes in grain size and bed thickness. The strata are generally interpreted to have formed in fluvial-deltaic environments (Stacher, 1995; Doust and Omatsola, 1990). The Agbada Formation underlies the Benin Formation and consists of interbedded fluvio-marine sands, sandstones and siltstone of various proportion and thickness representing the cyclic sequence of the off-lap unit (Weber, 1987). Texturally the sandstone varies from coarse to fine-grained, poorly to very well sorted, unconsolidated to slightly consolidated. Lignite streak and limonite coating occur with some shell fragments and glauconites (Short and Stauble, 1967). The shales are medium to dark grey, fairly consolidated and silty with localized glauconites. Shaliness increases downward and the formation pass gradually into the Akata formation. The Agbada Formation constitute a complex series of deposits laid down under at least five sub environments of deposition including holomarine, Barrier bar, barrier foot, Tidal coastal plain and lower deltaic flood plain (Whiteman, 1982). The thickness ranges from 0-4500m.

The Benin Formation comprises the top part of the Niger Delta clastic wedge and described as the coastal plain sands which outcrop at the Benin-Onitsha area in the north to beyond the present coastline (Short and Stauble, 1967). The top of the formation is the current subaerially exposed delta top surface and its base is defined by the top of the youngest underlying marine shales, extends to a depth of about 1400m. The age of the formation is thought to range from Oligocene to Recent (Short and Stauble, 1967). Shallow parts of the formation are composed entirely of non-marine sands deposited in the alluvial or upper coastal plain environment during progradation of the delta (Doust and Omatsola, 1990). The formation thins basinward and ends near the shelf edge. The deposit is predominantly continental in origin and consist of massive, highly porous, fresh water-bearing

sandstones with localized clay drapes and little shale intercalation which increases toward the base of the formation. Texturally, it consists of fine-grained sand and commonly granular. The grains are sub-rounded to well rounded, poorly sorted and partly unconsolidated. The sands are white or yellowish-brown due to limonitic coat. Plant remains and lignite streak occurs in places, with hematite and feldspar grain (Weber, 1987). It ranges from Miocene – Recent in age; although the lack of faunal content makes it difficult to date directly. The thickness ranges from 0 -2100m (Short and Stauble, 1967). It is thickest in the central area of the delta where there is maximum subsidence. The Benin formation is partly marine, partly deltaic, partly estuarine and partly lagoonal or lays down in a continental upper deltaic environment (Short and Stauble, 1967).

The modern Niger Delta is a mixed wave, tide and fluvial deltaic system. The delta is reworked by wave action along an arcuate coast with barrier islands, back-barrier lagoons, and channel ridges. Thick mangroves border the coastline of the lower Niger Delta plain. Incised into this coastline are numerous tide-dominated coastal estuaries, that have gradually been filled with sediment following the Holocene sea-level highstand. The modern delta front and the continental slope is characterized by localized slumps and canyons that bypass sediments into deeper waters. Although details of deltaic features are difficult to decipher within reservoir intervals of Niger Delta deposits, the modern distribution of distributary channels, estuary fills, shoreface, back-barrier lagoonal sediments, and delta plain deposits are assumed to be a good analogue.

It can be seen that the Niger delta has been affected by different episodes of progradation, retrogradation and aggradation as can be seen in the different sedimentation and especially in the Agbada formation.

The Benin formation has been affected by a long period of progradation coupled with a regressive phase of the sea thereby creating accommodation space for deposition of continental clastics from the hinterland into the delta.

Aggradational and parallel sequences of the Agbada formation are short-lived phases between the transgressive phase and regressive phase of the sea thereby creating a non-dominance stacking pattern in area where the sand to shale ratio is 50 per cent. However, with the increasing dominance of the transgressive phase, the sand to shale ratio begins to reduce abruptly as more marine sediments tend to deposit and move towards the shores.

In the continental slope and a little bit beyond the clastic wedge of the Niger delta sedimentary pile lies the pro-delta of the Akata. Incised valley cut on the continental slope can create channels by which turbulent turbidity currents can move sediments down the slope by gravity and sediments settles out by gravity in a turbidite sequence. Therefore the upper part of the Akata formation has lots of these isolated turbidite channel sand bodies underlain by continuous marine shale. These sand bodies are the objects for prospectivity in Niger delta deep water explorations.

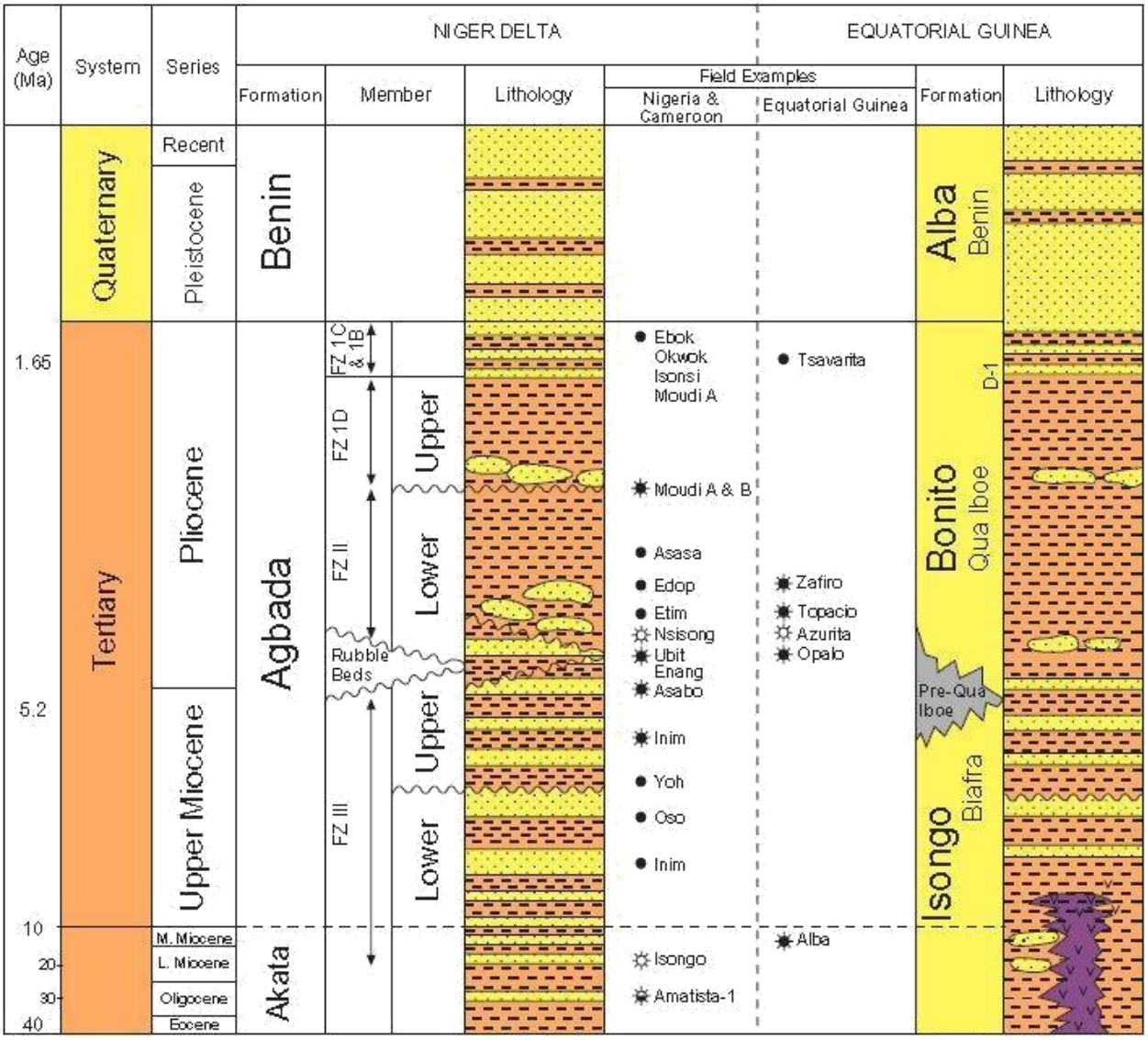

Fig 3.Niger – Delta structural setting (Doust and Omatsola, 1996) and Lauferts (1998)

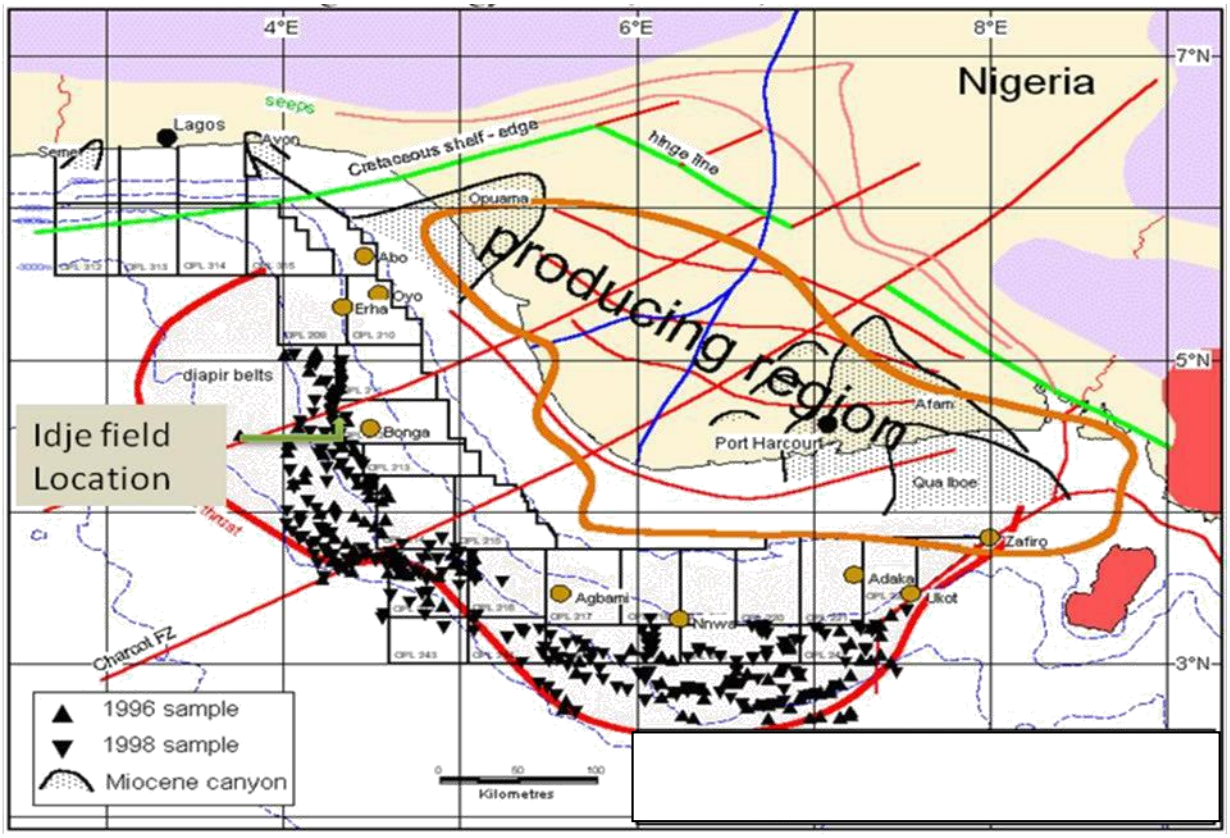

Fig. 4 Niger Delta and Equatorial Guinea Stratigraphic Build up. (Modified from Equatorial Guinea Ministry of Mines and Hydrocarbon)

2. MATERIALS AND METHODS

2.1 Data Overview

Idje field is located 70km southwest of Warri at the western lobe of Niger Delta. It lies within the proximal part of the deep offshore depobelt. The data used for this research include four wireline logs (gamma-ray, resistivity, neutron and density) cutting across the same reservoir for ten wells in the field. The data set was obtained in ASCII format in softcopy. It was then uploaded in Schlumberger PETREL 2009 to generate continuous logs for the different wells. The reservoir properties were plotted with the use of Golden software SURFER 9 which gave contours by krigging techniques and also generated 3-D surfaces for the reservoir top.

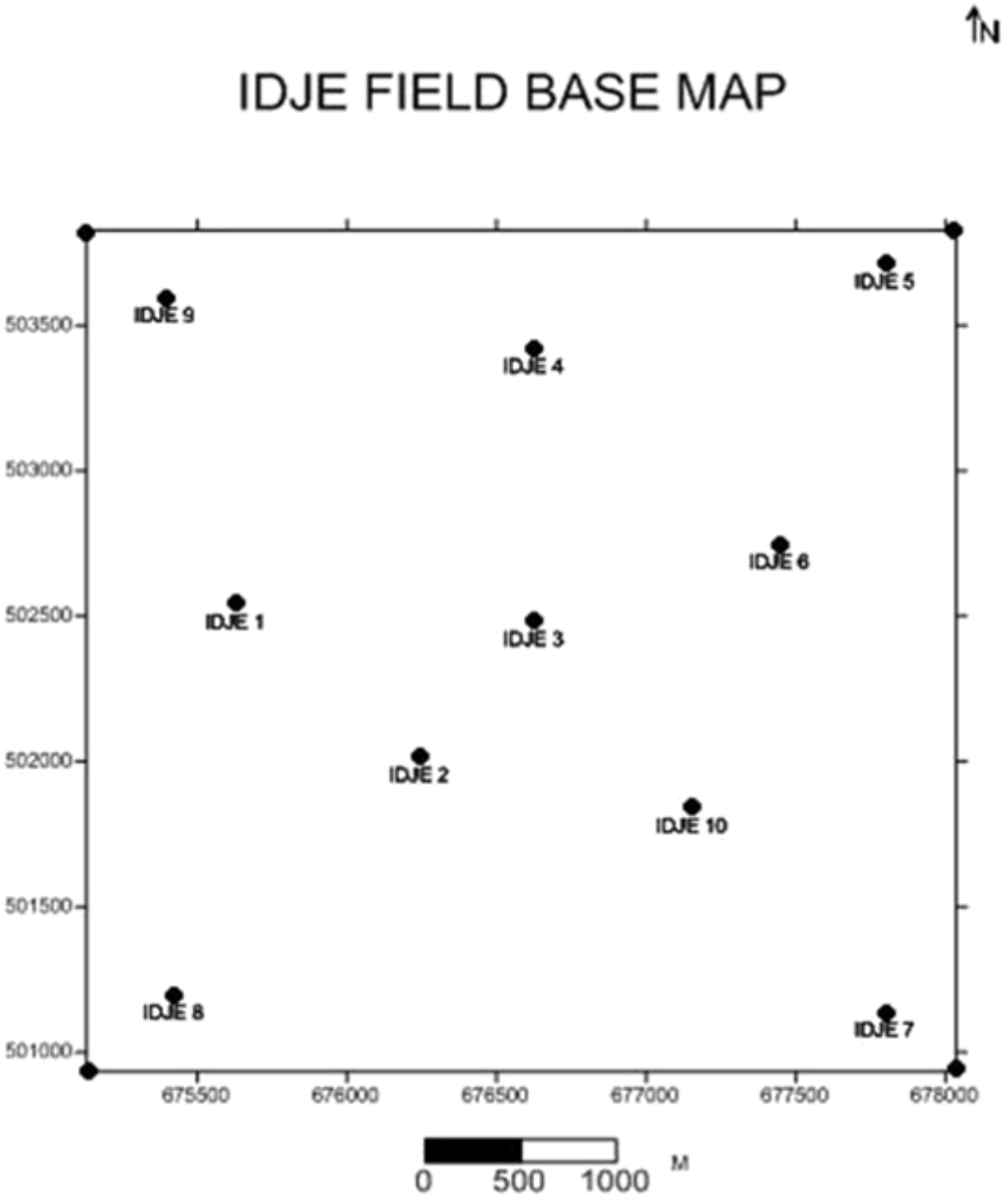

Fig. 5 IDJE FIELD BASE MAP IN UTM COORDINATES

2.2 Field Architecture.

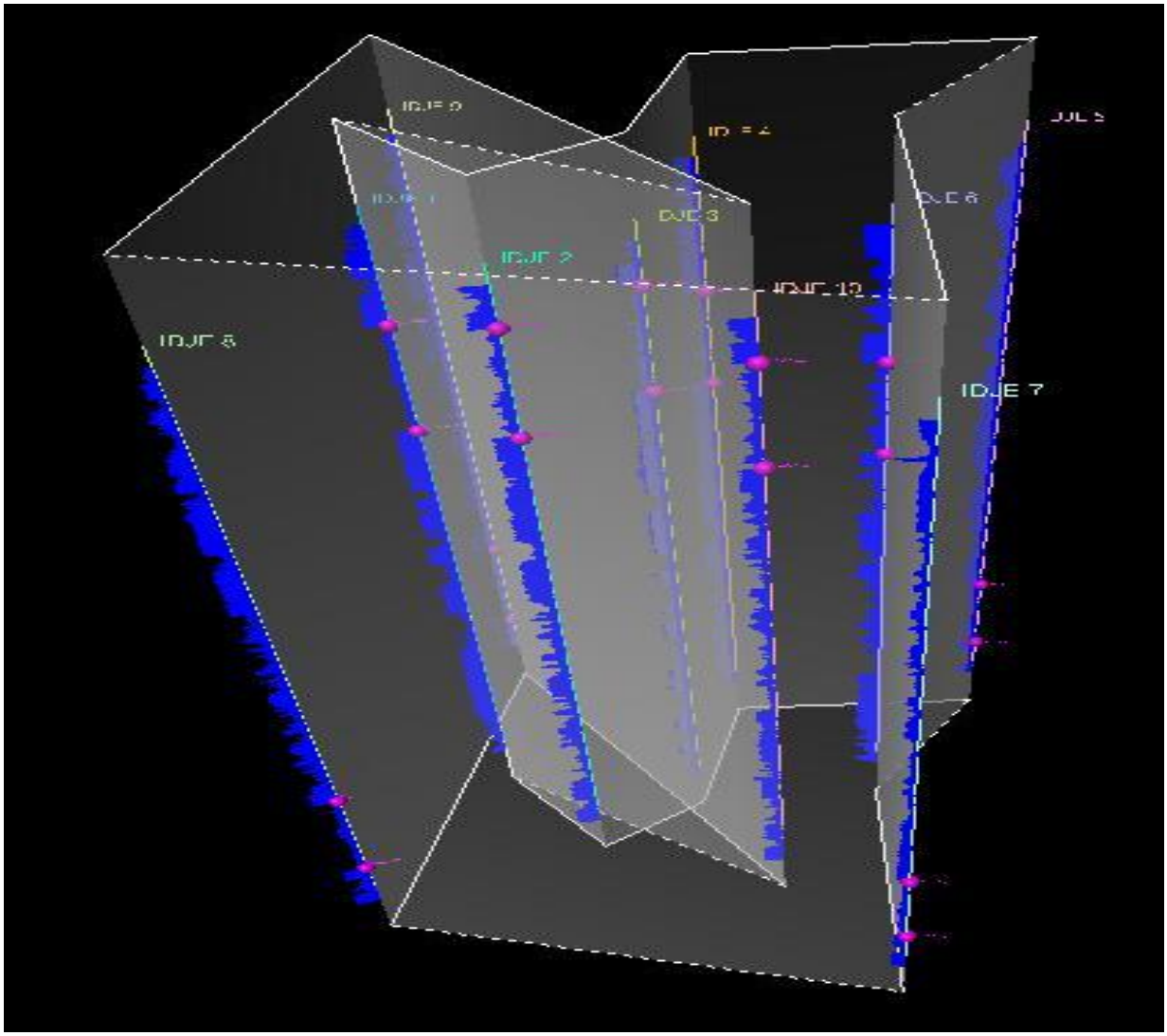

Fig. 6 structural dome architecture of the field

2.2 Well Logs

Well logs are graphical measurements acquired by instruments lowered down a borehole on a wireline cable or drill pipe during or after drilling operation. During acquisition, most measurements are made continuously whilst the instruments are moving. The resulting log of the measurements comprises a uniformly sampled set of data that is plotted against depth. Logs are an objective dataset that shows how specific measurements vary within and between formation units. Well logs here for petrophysical analysis could be obtained from LWD (logging while drilling) data or from wireline logging data that could be cable conveyed or pipe conveyed.

2.2.1 Gamma-Ray Log

The gamma-ray logging device consists of an electrically operated, downhole counter that detects naturally occurring gamma rays. The gamma rays are detected as pulses that are transmitted to the

surface where they are converted to electrical voltages and recorded continuously on film as the sonde is pulled up the hole. The

rays are emitted by the unstable elements uranium, thorium, and potassium, which are found in measurable amounts in all rocks. Shale generally contains the greatest concentrations of these elements and typically is more radioactive than sandstone, limestone, dolomite, salt, or anhydrite. Gamma-ray logging is thus highly useful in distinguishing shale from other rock types. Gamma-ray recording equipment is usually designed so that the curve deflects toward the right as radioactivity increases. On the gamma-ray log, the deflection to the extreme right indicates shale. The parts of the curve with less deflection indicate non-shale lithologies such as sandstone and limestone. The gamma-ray log is used principally for bed definition, correlation, and determination of lithofacies because of its shale-distinguishing characteristic. The high penetrating power of gamma rays permits logging in cased or uncased holes, regardless of the nature of the fluid, if any, in the hole. The log is commonly calibrated from 0 to 150 API on a linear scale.

2.2.2 Resistivity Log

The resistivity log records the resistivities of subsurface formations and any fluids they may contain. Its design is based on electrical theory and instrumentation. The resistivity of the rock formation must be measured in the uncased portion of the borehole. Current and measuring electrodes are mounted on a mandrel or sonde and lowered down the hole. Different spacing between electrodes allows resistivity measurements at different distances from the borehole into the rock formation. A short spacing between electrodes gives a radius of investigation of only a few inches into the formation; longer spacing measures a larger radius. Three simultaneous resistivity measurements (micro, shallow and deep), using different electrode spacing, are usually recorded. The resistivities at different radii of penetration are compared to indicate the true resistivity, which is modified to varying degrees near the borehole by the invasion of the drilling mud into the rock and the influence of the borehole itself. The resistivity logs are calibrated on a Logarithmic scale in ohmmeters. High resistivity values are a direct indication of hydrocarbon-bearing intervals. Gas and condensate resistivity values are relatively higher than those of oil. However, resolution of fluid contact based on resistivity alone could be quite erroneous.

2.2.3 Neutron Log

The neutron log consists of an americium-beryllium or plutonium-beryllium source that emits fast neutrons, and a radiation detector placed close to the source. The emitted neutrons are electrically neutral particles that proceed outward from the source and penetrate the adjacent rocks until they

are captured by the atomic nuclei of certain elements after several collisions. When the neutron is captured, it is absorbed and one or more high-energy gamma rays are emitted. The induced gamma rays are of greater intensity and quantity than the naturally occurring gamma rays, thus permitting the measurements of the induced radiation without interference from the relatively weak, natural radiation. The atomic nucleus most successful in slowing down the emitted neutron is the hydrogen nucleus which has a mass almost identical to the neutron. When the hydrogen concentration is large, most of the neutrons are slowed down and captured within a short distance. Due to the source-detector spacing commonly used, a high concentration of hydrogen allows only a few gamma rays to reach the detector. Because hydrogen is a common component of formation fluids, and rocks must be porous to contain these fluids, the intensity of the induced gamma rays indicates the amount of fluid and porosity. High intensity generally signifies non-porous rock, whereas low intensity signifies porous, fluid-bearing beds. Neutron is used to bombard the formation and the induced gamma-ray from the bombardment is measured. The presence of hydrogen atoms tends to absorb the neutrons giving less room for gamma-ray induction thus leading to low count rate. Shale generally shows a high porosity on a neutron log because of the hydrogen chemically combined in its

molecules or present in water in its pores. The porosity, however, is not "effective porosity", as the voids are not interconnected, and shale is usually impervious. Natural gas, which contains less hydrogen than oil or water, gives a higher counting rate and the neutron curve records low, inaccurate porosity. The primary use of the neutron log is for porosity determination. It is also useful for delineation and correlation of formations. The log, like the gamma-ray log, can be made in either cased or uncased holes and requires no fluid. When used with the gamma-ray, the neutron log may provide a quantitative record of shale and indicate porous and non-porous rock. Thus, it is particularly helpful in cased wells, for surveying old wells and doing "work-over" jobs. Gas containing rocks may also be indicated. It is of interest to know here that neutron log only resolves the liquid-filled pore spaces and give abnormally low porosity value for gas-filled spaces. The neutron porosity could be calibrated in fractional porosity or terms of percentage porosity. This work puts the fractional porosity calibration into consideration. It is calibrated from 0.7 on the left to 0 porosity units on the right i.e. it decreases to the right.

2.2.4 Density Log

The density log is acquired with a radioactivity tool based on the response of the rock to induced, medium-energy gamma rays. The result is an approximate measurement of the bulk density of the rock. The bulk density, as used in well logging, is the number of grams or mass weight of a substance divided by its volume. The tool consists of a gamma-ray source and a detector mounted

on a skid that is in contact with the borehole wall. Gamma rays, which are emitted by the source, are transmitted through the formation. The number that reaches the detector depends on the abundance of electrons within the rock material. If many electrons are present, the gamma rays are quickly absorbed and only a few are counted. Conversely, if the electrons are few, many gamma rays are counted. An increase in counting rate, therefore, indicates a decrease in bulk density. Gamma-ray

from radioactive source is used to bombard rock and the reflected and diffused gamma-ray is counted. Electrons tend to absorb the gamma-ray and thus giving less count in the reflected gamma-ray. The density log responds to electron density, but because the two densities are so closely related, the log is scaled in bulk density. Shales have a higher electron density than sand and thus its presence yields fewer counts than sand. The important relationship between the electron density as recorded by the density log and the porosity of a formation is simple and direct. A formation with a considerable amount of open space offers little resistance to the progression of medium-energy gamma rays. Therefore, rock with good porosity has a low electron and bulk density, as indicated by a high count of diffused gamma rays. The density log provides another method of direct porosity measurement. Oil and gas are less dense than water, which results in a lower density reading, and therefore, unlike a neutron log, their presence causes an indication of favourable porosity. When used to estimate effective porosity, the density log is not influenced as strongly by shale as the neutron log. The density log is calibrated from left to right and increases towards the right. The calibration used for this study is from 1.65 to 2.65 g/cc.

2.3 petrophysical analysis

This involves the use of empirical formulae to estimate the petrophysical properties of the D-3 reservoir. The D-3 reservoir which was identified through the use of the electrofacies signatures were further characterized quantitatively to arrive at these petrophysical parameters. Some of these parameters are discussed below:

2.3.1 Storage Volume

This is the capacity to store hydrocarbon in the reservoir. The storage volume is always higher than the hydrocarbon pore volume within a well because the net pay zone is inclusive of the grain matrix whereas, the grain matrix is absent in the hydrocarbon pore volume computation as only the hydrocarbon in the pore spaces is calculated for.

$$\text{Storage Volume} = \phi_{N\text{-}D} * \text{Net Pay Thickness} \qquad (1)$$

2.3.2 Volume of Oil Resources

This is the volume of oil resources per unit acre in a field. It could be used to estimate oil reserve volume in the field.

$$\text{Volume of Oil Resources} = (7758*h*HCPV)/B_o \qquad (2)$$

Where h = net pay oil, B_o = Formation oil volume factor = 1.2 bbls/STB

2.3.2 Volume of Gas Resources

This is the volume of gas resources per unit acre in a field. It could be used to estimate gas reserve volume in the field.

$$\text{Volume of Gas Resources} = (43560 * h * HCPV)/B_g \qquad (3)$$

Where h = net pay gas, B_g = Formation gas volume factor = 0.005 cuft/scf

2.3.3 Volume Of Oil Originally In Place

Oil originally in place is computed with the following equation:

$$\text{OOIP} = \text{Volume of Oil Resources} * \text{Area covered by oil} \qquad (4)$$

Here, recovery factors have not been applied. This volume could be calculated directly from the volume of oil resources contour map. The area of the map occupied by oil is calculated sectionally concerning the contour intervals. The individual area is then multiplied by the individual contour value to get the individual volumes. Finally, all the individual volumes are added to get the total volume of oil resources in the field which is equivalent to the volume of oil in place. The unit here is stock tank barrels.

2.3.4 Volume Of Gas Originally In Place

This is calculated the same way as that of oil originally in place from the volume of a gas resources contour map. The unit here is standard cubic feet.

GOIP = Volume of Gas Resources * Area covered by gas (5)

2.3.5 Direct Measurement Of Hydrocarbon In Place

The hydrocarbon originally in place could also be computed directly using the average value for the net pay thicknesses, average hydrocarbon saturations, and average porosity values and substituted in the following equations:

$$OOIP = (7758*A_{oil}*h_{oil}*s_{h(oil)}*\phi_{N-D})/b_o \quad (6)$$

$$OGIP = (43560*A_{gas}*h_{gas}*s_{h(gas)}*\phi_{N-D})/b_g \quad (7)$$

A_{oil} = Area occupied by oil

A_{gas} = Area occupied by gas

h_{oil} = Average height of oil column

h_{gas} = Average height of gas column

$s_{h(oil)}$ = Hydrocarbon saturation (oil column)

$s_{h(gas)}$=Hydrocarbon saturation (gas)

NOTE: $1Km^2 = 247.104$ Acres

3. RESULTS

3.1 Petrophysical Results

The different petrophysical parameters computed for the D-3 reservoir are tabulated below:

Table 1. Petrophysical parameters

	IDJE 1	IDJE 2	IDJE 3	IDJE 4	IDJE 5	IDJE 6	IDJE 7	IDJE 8	IDJE 9	IDJE 10
GR_I	0.1	0.25	0.34	0.23	0.31	0.29	0.24	0.06	0.08	0.32
V_{SH}	0.03	0.09	0.14	0.08	0.13	0.12	0.09	0.02	0.02	0.13
POROSITY (Ø)	0.26	0.25	0.24	0.26	0.25	0.25	0.26	0.26	0.26	0.24
F	11.63	12.41	12.22	11.3	11.06	11.17	11.38	11.42	11.44	12.09
$R_{w\ \Omega m}$	0.1	0.09	0.09	0.1	0.1	0.1	0.1	0.1	0.1	0.09
S_w	0.71	0.21	0.21	0.94	0.94	0.89	0.97	0.97	0.97	0.18
S_{hc}	0.29	0.79	0.79	0.06	0.06	0.11	0.03	0.03	0.03	0.82
BVW	0.18	0.05	0.05	0.24	0.25	0.22	0.25	0.25	0.25	0.04
S_{wirr}	0.08	0.08	0.08	0.07	0.07	0.07	0.07	0.08	0.08	0.08
K mD	3516.94	2592.36	2564.57	3772.93	3737.13	3682.04	3820.48	3840.05	3854.89	2555.47
HCPV	0.08	0.2	0.19	0.02	0	0.03	0.01	0.01	0.01	0.2

TOP DEPTH ft	9410	9163	9170	9570	11262	9555	11251	11159	11188	9168
GOC ft	-	9381	9381	-	-	-	-	-	-	9381
OWC ft	9584	9584	9584	9584	-	9584	-	-	-	9584
BOTTOM DEPTH ft	9897	9613	9610	10011	11663	9977	11648	11649	11680	9598
GROSS THICKNESS ft	487	450	440	441	401	422	397	490	492	430
NET PAY THICKNESS ft	174	421	414	14	-	29	-	-	-	416
TOTAL V_{SH}	14.61	40.5	61.6	35.28	52.13	50.64	35.73	9.8	9.84	55.9
NET THICKNESS ft	472.39	409.5	378.4	405.72	348.87	371.36	361.27	480.2	482.16	374.1
N/G RATIO	0.97	0.91	0.86	0.92	0.87	0.88	0.91	0.98	0.98	0.87
POROSITY EFFECTIVE	0.25	0.23	0.21	0.24	0.22	0.22	0.24	0.25	0.25	0.21
STORAGE VOLUME	45.24	105.25	99.36	3.64	-	7.25	-	-	-	99.84
VOL OF OIL RESOURCES	89992.8	262479	249355.05	1810.2	-	5624.55	-	-	-	262479
VOL OF GAS RESOURCES	-	379843200	349264080	-	-	-	-	-	-	371131200

3.2 Field architecture

From Fig. 6 above, the wells at the flanges of the map areas have the D – 3 reservoirs at the bottom of the wells whereas those at the central portion of the map area have the D-3 reservoir at the top of the wells. This indicated that the reservoir has structural dome architecture.

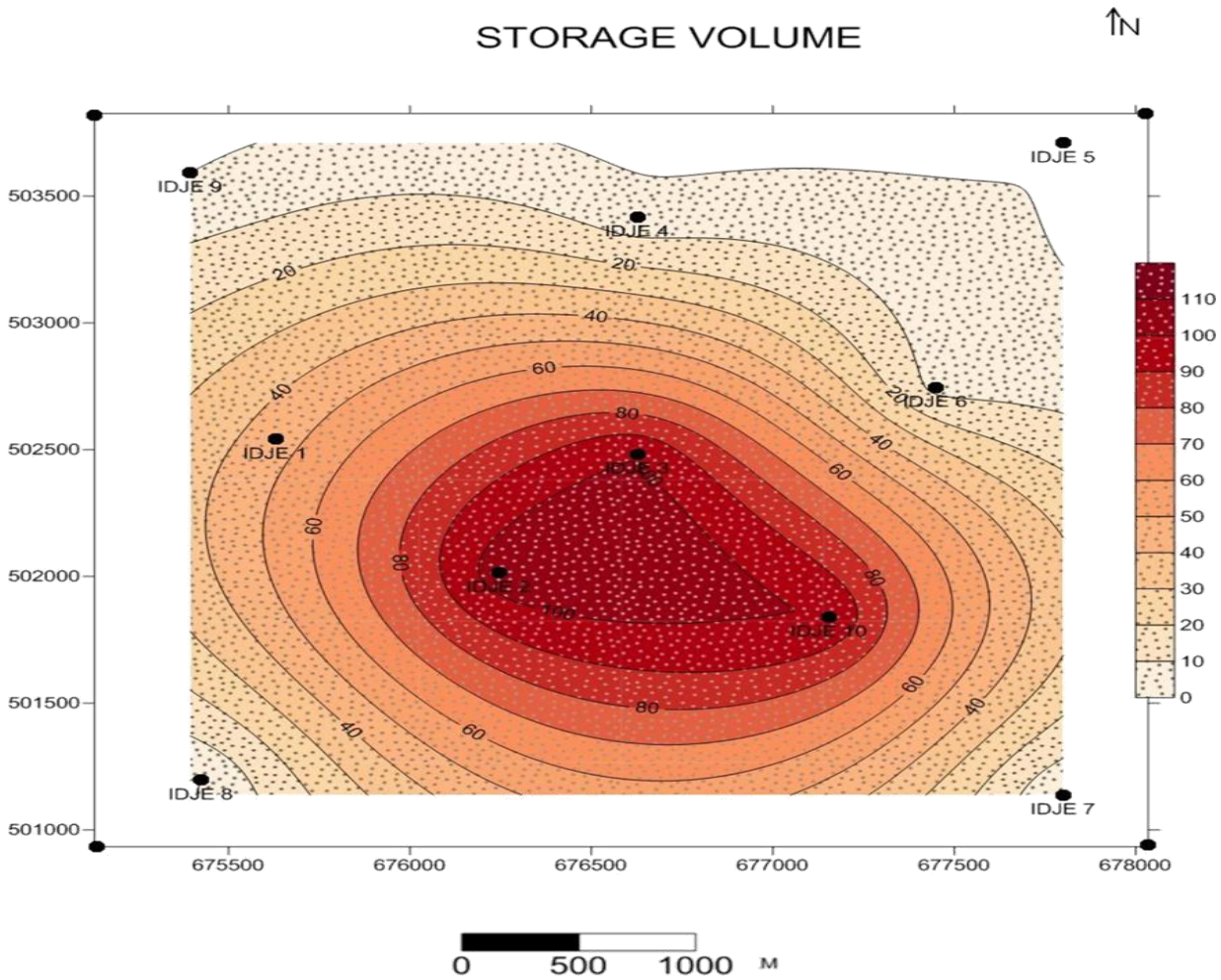

Fig. 7 Hydrocarbon Storage Volume Contour

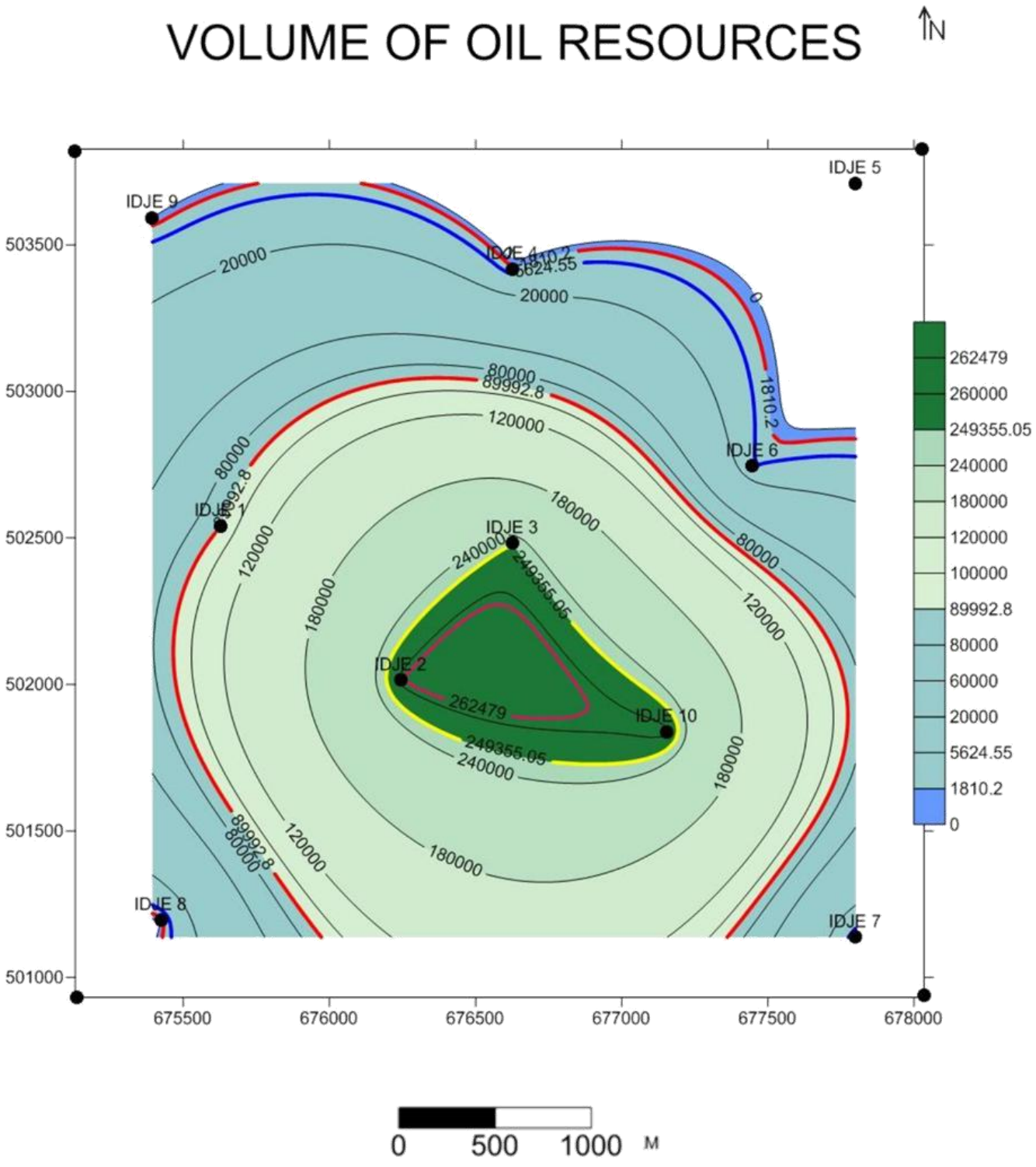

Fig .8 Volume of Oil Resources Contour

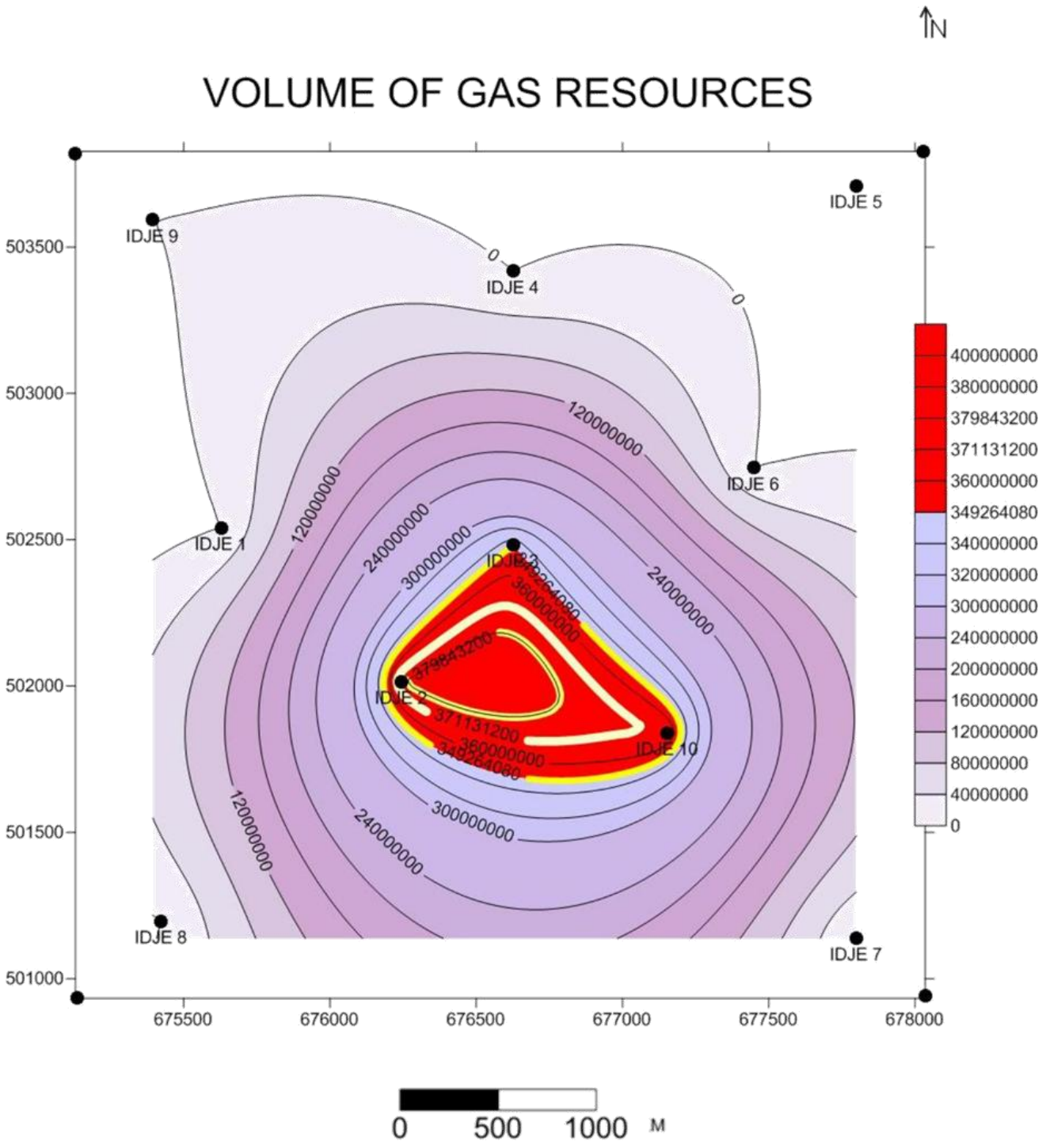

Fig. 9 Volume of Gas Resources Contour

3.3 Volumetric Method for Hydrocarbon Reserve Estimation Of The D-3 Reservoir.

Volumetric methods attempt to determine the amount of oil in place by using the size of the reservoir as well as the physical properties of its rocks and fluids, then a recovery factor is assumed, using assumptions from fields with similar characteristics. OOIP is multiplied by the

recovery factor to arrive at a reserve estimate. The recovery factors for gas cap fields (typical of Idje field) is usually in the range from 15 - 25 % (Ivan Sandrea and Rafael Sandrea, 2007) for solution gas drive, gas cap drive and water drive saturated reservoirs and is usually the first estimate for a discovery until other production mechanisms have been observed in the field. A simple weighted average among the major oil provinces gives an average recovery factor of 22% which is well within the range of the solution gas drive reservoirs. By analogy, the overall recovery factor for the bulk of the world's conventional oil reserves would at best be about 20% (Ivan Sandrea and Rafael Sandrea, 2007). For the sake of this study however, a recovery factor of 20% is employed.

The oil reserve and gas reserve could be computed from the formulae below:

$$\text{Oil Reserve} = (7758 * A_{oil} * h_{oil} * s_{h(oil)} * \phi_{N\text{-}D}) / b_o * R_o \quad (7)$$

$$\text{Gas Reserve} = (43560 * A_{gas} * h_{gas} * s_{h(gas)} * \phi_{N\text{-}D}) / b_g * R_o \quad (8)$$

R_o = Recovery factor (fractional) $\phi_{N\text{-}D}$ = Porosity (fractional)

A_{oil} = Area occupied by oil A_{gas} = Area occupied by gas

h_{oil} = Average height of oil column h_{gas} = Average height of the gas column

$s_{h(oil)}$ = Hydrocarbon saturation (oil column) fractional.

$s_{h(gas)}$=Hydrocarbon saturation (gas) fractional.

B_o = Formation oil volume factor = 1.2 bbls/STB B_g =

Formation gas volume factor = 0.005 cuft/scf

4. DISCUSSION

Reserve is computed for individual intervals before subsequent addition. This estimate is strictly for the volume of oil originally in place and exclusive of the recovery factor for the field. The gas reserve (Fig. 9) followed a similar trend as the oil reserve. It is interesting to note here that recovery factors have also not been applied. This estimate is for GOIP.

Calculated Area of gas reserve = 1.736km2 = 428.932 acres

Calculated Area of oil reserve = 2.997km2 = 740.572 acres

The average height of gas column = 214ft

Average height of oil column = 137.67ft

Average hydrocarbon saturation in oil column = 0.48

Average hydrocarbon saturation in gas column = o.8

Average porosity = 0.25

Oil reserve estimate therefore = (7758*740.572*137.67*0.48*0.25)/1.2*0.2

= 15,819,267.55 barrels

= approximately 15.8 million barrels.

Gas reserve estimate is = (43560*428.932*214*0.8*0.25)/0.005*0.2

= 31,987,483,800 cubic feet

= approximately 32 billion cuft

The oil reserve in the D-3 reservoir is 15.8 million barrels while the gas reserve is 32 billion cubic feet.

5. CONCLUSION

The volumetric reserve estimate for the D-3 reservoir shows that it contains 15.8 million barrels of oil and 32 billion cubic feet of gas. If the field is produced at the rate of 10,000 barrels per day, it would yield production for approximately 4 years before subsequent secondary and tertiary recovery measures would be employed. This work could be used as an input tool for pre-existing models to generate excellent dynamic simulations for optimum productivity. The volume of oil and gas resources contours could be used as a predictive model to estimate hydrocarbon reserve potentials for proper field management. The volumetric reserve estimate could be used to evaluate reserve economics and producibility rate to ascertain possible duration before field abandonment. This work could also be incorporated into several multi-disciplinary projects that use integrated subsurface datasets (core, wireline log, 3D seismic and production data), insights from outcrop analogues and novel modelling techniques to characterize geology and fluid flow in hydrocarbon reservoirs.

COMPETING INTERESTS

Authors have declared that no competing interests exist

REFERENCES

1. Short, K.C, and A.J. Stauble, 1967: Outline of Geology of Niger Delta: American Association of Petroleum Geologists, Bulletin, v.51, p.761-779.

2. Avbovbo, A.A, 1978. Tertiary lithostratigraphy of Niger Delta: Amer. Assoc.
3. Petrol. Geol . Bull., V. 62, p 295-306.

4. Weber, K.J, and Daukoru, E.M, 1975, Petroleum Geology of the Niger Delta: Proceedings of the Ninth World Petroleum Congress, volume 2, Geology: London, Applied Science Publishers Ltd., p.210-221.

5. Evamy, B. D; Haremboure, J; Kamerling, P; Knaap, W.A; Molloy, F.A; and Rowlands, P.H, 1978: Hydrocarbon habitat of Tertiary Niger Delta: American Association of Petroleum Geologists Bulletin, v.62, p. 77-298.

6. Doust, H, and Omatsola, E, 1990, Niger Delta, in, Edwards, J.D., and Santogrossi, P.A., eds., Divergent/passive Margin Basins, AAPG Memoir 48: Tulsa, American Association of Petroleum Geologists;p.239-248
7. Reijers, T.J.A; S.W, Petters, and C.S, Nwajide, 1997: The Niger Delta Basin, in R.C. Selley, ed., African Basins-Sedimentary Basin of the World 3, Amsterdam, Elsevier Science,p.151-172.

8. Tuttle, W.L.M; Charpentier, R.R; and Brownfield, M.E, 1999: The Niger Delta petroleum system; Niger delta province, Nigeria, Cameroon and Equatorial Guinea, Africa USGS. Denver, Colorado, open file report, world energy project.

9. Weber, K.J, 1987: Hydrocarbon distribution patterns in Nigerian growth faults structures controlled by structural styles and stratigraphy: Journal of Petroleum Science and Engineering. V. 1, p. 91 – 104.

10. Whiteman, A, 1982, Nigeria: Its Petroleum Geology, Resources and Potential: London, Graham and Trotman, p. 110 – 160.

11. Stacher, P, 1995 . Present Understanding of the Niger Delta hydrocarbon habitate. In: M. N Oti and G. Postman Eds. Geology of Deltas. AA Balkema, Rotterdam. Pp 257 – 267.

12. Lauferts H., 1998. Deep offshore West Niger Delta slope, Nigeria – scale and geometries in seismic and outcrop indicating mechanisms for deposition. Extended Abstracts Volume. 1998 AAPG International Conference and Exhibition, November 8-11, 1998 Rio de Janeiro, p. 18-19.

13. Ivan Sandrea and Rafael Sandrea, 2007: Global Oil Reserves – Recovery Factors Leave Vast Target for EOR Technologies. Oil & Gas Journal. Part 1 and 2